

Design and Build of Swarm Quadrotor UAVs at UGS

Alvin Ng, Qiwang Foo, Ridhwan Jumat, Tony Rayar Victor, Wei Chong Koh, Sutthiphong Srigrarom
 University of Glasgow Singapore
 Contact e-mail: spot.srigrarom@glasgow.ac.uk

ABSTRACT

At the University of Glasgow, we have been developing the swarm of autonomous micro- unmanned aerial vehicle (μ -UAVs), as a part of team projects of the final year project design course: Aerospace Systems Design Project 4 for our BEng in Aerospace Systems program. For our Singapore campus, where similar course is conducted, the platform chosen is the quadrotor. In this paper, we present the conceptual design, construction, flight test, swarm behaviour and lessons learnt.

1. INTRODUCTION

A Quad-rotor consists of four motors with a rotor attached to each. When the rotor spins, it generates lift vertically. Lift increases when the rotor spins faster and vice versa. Hence Quad-rotor's climb and descent is dependent on the speed of the rotor. In order to hover, the sum of lift produced by the 4 rotors must be equivalent to the gravitational force.

Manoeuvring along the horizontal plane is achieved by tilting the Quad-rotor in the desired direction. The difference in the Lift between the rotors causes tilting. The horizontal component of lift results in movement along horizontal plane.

If all rotors spin in clockwise direction, the Quad-rotor will spin undesirably in the opposite direction. To prevent this the alternate rotors spin in opposite direction. Therefore the effect of the torque generated by the two opposing pairs of spinning rotors is balanced when all rotors are rotating with equal speed. In Quad-rotor flight, the moment of the vehicle is determined by its velocity, angle of attack, and its airframe. It has to be considered because they affect the attitude control, and thrust variation of the rotorcraft.

2. QUADROTOR MODELLING

2.1 Frame of references

The Quad-rotor is modelled in a Flat Earth coordinate reference. Flat Earth reference neglects the centrifugal and Coriolis accelerations since the trajectory of vehicle is much slower than the orbital speed. This section discuss about the dynamics equations of motion of the Quadrotor and how it was transformed into the Flat Earth Frame of Reference.

Frame of reference denoted as (x, y, z) axes is simply an axes system which is used to define quantities or measurements. The axes can be fixed to a body or earth. In this case, the body axes (x_b, y_b, z_b) is rotating with respect to the centre of gravity of the

quad-rotor and the earth axes (x_e, y_e, z_e) is with respect to the earth as shown on Fig 1.

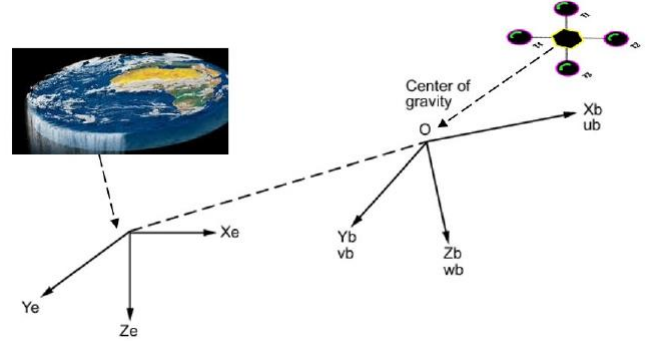


Fig. 1 Flat Earth Reference Frame

Relationship between the quad-rotor's frame of reference and the earth's frame of reference can be expressed by a transformation matrix as shown below. Such matrix is obtained using the three Euler angles commonly used in an aircraft in a prescribed sequence of rotation of roll, pitch and yaw.

$$\begin{bmatrix} x_b \\ y_b \\ z_b \end{bmatrix} = \begin{bmatrix} c\theta c\psi & c\theta s\psi & -s\theta \\ -c\phi s\psi + s\phi s\theta s\psi & -c\phi c\psi + s\phi s\theta s\psi & s\phi c\theta \\ s\phi s\psi + c\phi s\theta c\psi & s\phi c\psi + c\phi s\theta s\psi & c\phi c\theta \end{bmatrix} \begin{bmatrix} x_e \\ y_e \\ z_e \end{bmatrix}$$

where s, c denote sine and cosine functions respectively.

2.2 Equations of motion

As forces are produced by the total thrust of the rotor in the negative z direction and gravity is acting on the quad-rotor in the positive z direction, to transform forces from the body frame of reference to the earth frame of reference, the transformation matrix is used and therefore resulting in the following translational equations

$$\begin{aligned} \ddot{x} &= -\frac{U}{m} (\cos\psi \sin\theta \cos\phi + \sin\psi \sin\phi) \\ \ddot{y} &= -\frac{U}{m} (\sin\psi \sin\theta \cos\phi - \cos\psi \sin\phi) \\ \ddot{z} &= -\frac{U}{m} (\cos\theta \cos\phi) + g \end{aligned}$$

For rotational motion, J is the inertia matrix which is calculated by assuming rotors as individual point mass located

at a distance away from the quad-rotor's central hub. The hub is considered as a dense sphere with radius and mass at the center as shown on Fig. 2.

Therefore,

$$J_x = J_y = \frac{2MR^2}{5} + 2ml^2 \quad \text{and} \quad J_z = \frac{2MR^2}{5} + 4ml^2$$

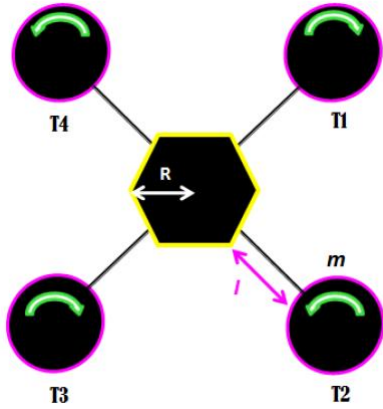


Fig. 2 Quad rotor dimensions

The equations of rotational motion are

$$\ddot{\phi} = \frac{1}{J_x} \tau_\phi \quad \ddot{\theta} = \frac{1}{J_y} \tau_\theta \quad \ddot{\psi} = \frac{1}{J_z} \tau_\psi$$

2.3 Dynamics of motor

Since thrust for the quad-rotor are produced by the rotors, it is important to consider the dynamic of the motor when modelling the quad-rotor. The DC-motor is able to convert electrical energy to mechanical energy. With a given voltage input, the rotational speed of a motor can be calculated as shown below.

$$V_{in} = R_m i + L_m \frac{di}{dt} + k_e \dot{\Omega} \quad \text{where} \quad \dot{\Omega} = \frac{k_m i}{J_m}$$

By integrating $\dot{\Omega}$ to obtain Ω , the thrust generated can be calculated using the following set of equations.

$$C_t = \frac{T}{\rho n^2 D^4} \quad \text{where} \quad n = \frac{\Omega}{2\pi}$$

Therefore,

$$T = C_t \rho \left(\frac{\Omega}{2\pi} \right)^2 D^4$$

Finally, with the calculated thrust and measured, following flight performance can be determined.

$$\begin{aligned} U_1 &= T_1 + T_2 + T_3 + T_4 & (\text{hover}) \\ \tau_\phi &= l[(T_3 + T_4) - (T_1 + T_2)] & (\text{roll}) \\ \tau_\theta &= l[(T_1 + T_4) - (T_2 + T_3)] & (\text{pitch}) \\ \tau_\psi &= (T_1 + T_3) - (T_2 + T_4) & (\text{yaw}) \end{aligned}$$

3. QUADROTOR CONSTRUCTION

3.1 Structure

The Quad-Rotor platform was bought by UGs and given to us to assemble. The package comes with pieces of the quadrotor. The main structural components of our quad-rotor are summarized on the following table.



Fig. 3 Completed Structure of Quad-Rotor

Qty	Name	Dimension
1	Central Hub	155mm
4	Motor Arm	330mm
2	Stand	220mm

Central Hub

The central hub is made up of 2 carbon fibre sheets that are fastened together while leaving space for the motor arms to be secured to. The central hub also has an elevated platform for the placement of the ArduPilot Mega 2.5. The interior of the central hub holds all the wires such as the power module and the 4 to 1 conversion adapter. The Li-polymer battery is cable tied to the bottom of the central hub for better stability.

Motor Arm

The motor arms are made up of hollow carbon rod. These rods are securely fastened to the central hub using rubber spacers. This is to reduce the amount of vibrations caused by each motor. The rods are positioned to be equally spaced from each other. The motors are all seated on a carbon fibre sheets which are fastened together using bolts and nuts.

Stand

The stand is also made up of hollow carbon fibre rod. The part that is connected to the central hub is sandwiched between 2

carbon fibre sheets to strengthen the joints. The bottom stands are to provide more surface contact to the ground. It also allows the vehicle to have a more stable take off by enforcing it to be at an upright position.

3.2 Electronic Components

The electronic components used for our platform are summarized on the following table:

Qty	Name	Weight
4	ESC	32g
4	Brushless Motor	55g
1	Li-polymer Battery	250g
4	Plugs	1g
1	4 to 1 Conversion Adapters	3g
1	Power Module	3g
1	ArduPilot Mega 2.5	31g
1	Receiver	9.4g

Electronic Speed Controller (ESC)

The Electronic Speed Controller (ESC) chosen, is specially designed for multi-rotor motor. Each ESC weighs 32grams with the dimensions of 55mm by 26mm by 11.6mm (width by length by height). The brushless ESC provides variable power to the motor allowing proportional speed adjustments. This ESC also has a voltage cut-off function which lowers power when the voltage is low.

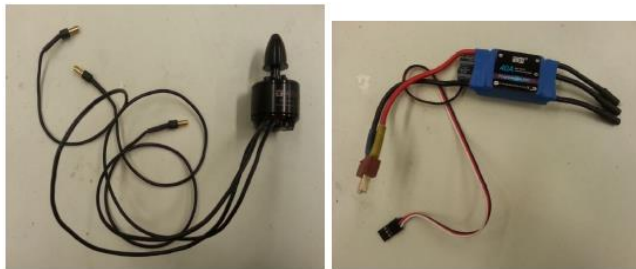


Fig. 4 Brushed ESC DYS OPTO-40A and Tiger Motor MT2212-13 - KV

Brushless Motor

The motors (Fig.4) used are out runner brushless. Outrunner motors have a lower speed however greater torque which allows us to direct drive a larger propeller without the use of a gearbox. Each motor weighs around 55grams with the dimensions of 27.5mm by 28mm (length by height) and can generate lift up to 800grams depending on the propeller used.

Batteries

The battery used is a 3 cell Lithium Polymer. It has a voltage value of 11.1V and current rating of 3300mAh. The higher the rating the longer it can provide power to the other electronic components. Since we are using 4 motors we require a strong battery however power has its price. The stronger the battery the heavier and bigger it is. For our case it sets us back to 250 grams and dimensions 43mm by 130mm by 13mm (width by length by height). The battery could last a maximum of around 10 to 15 minutes of flight time.



Fig. 5 RevoLectrix Li-polymer Battery

Plugs

The plugs are soldered to the output of the ESC to connect to the batteries which has a Dean plug female. It allows 40A current to pass through. This connector ensures secure connection while easy for plugging and unplugging.

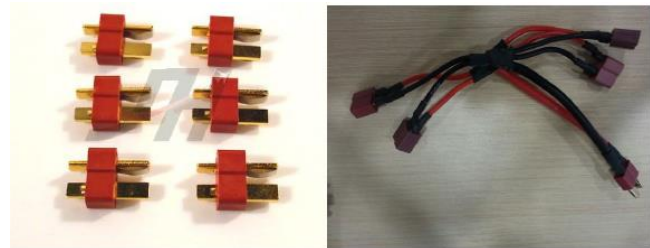


Fig. 6 Dean Plug male 4 Female to 1 male

4 to 1 Conversion Adapters

The 4 to 1 conversion adapters (Fig.6) are, 4 Dean Plug female to 1 Dean Plug male. The input for the female plug is the male plug soldered on the ESC wire. The output for the male plug of the adapter is to the battery. Only 1 adapter is required to power up the 4 ESC using 1 battery source.

Power Module

A power module has a 6-pos connector that provides +5.3V voltage and 2.25A current. It is needed as we need a connector to power the ArduPilot Mega. The power module accepts a maximum input voltage of 18V (up to 4S Lipo battery) and maximum current of 90Amps.

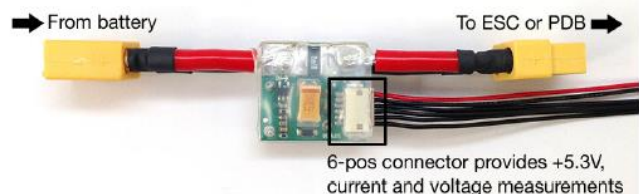


Fig. 7 Power Module

ArduPilot Mega 2.5

The ArduPilot Mega 2.5 is a complete open source autopilot system. The Ardupilot version that was used has a plug and play design, no assembly or programming is required. However there is a function to allow users to modify the programming codes using the Arduino software. The function of this devices is to turn any fixed, rotary wing or multicopter vehicle (even cars and boats) into a fully autonomous vehicle; capable of performing programmed GPS missions with waypoints.



Fig. 8 ArduPilot Mega 2.5
Fig. 9 AR 8000 DSMX 8 Channel

Receiver

The Receiver used is, 2.4GHz 8 channel. It comprises of a compact main receiver that is linked to an even smaller satellite receiver by a 6” lead, the AR 8000 acts as a pair of extremely sharp RF “eyes” that each take in a slightly different view of the signal environment. Information from both receivers is then processed by patent pending Spektrum software that takes information from each receiver and combines it to form the most vivid “picture” of an RF signal. Using 2.4GHz means that our receiver will not be interfered with other frequency unlike using crystals which could be interfered with when there are other flyers using the same frequency. After binding the receiver to the transmitter, it is forever bind to the particular transmitter which is why it will not interfere with others.

4. SIMULATION MODELS

Using the equations of motion derived earlier and the dimensions of the Quad-rotor constructed in previous section, a mathematical model is created and implemented on MATLAB Simulink. As Shown in Fig 17, the inputs for the quad-rotor simulation are the desired X-axis, Y-axis and Z-axis positions. The outputs are the linear and angular acceleration which will be integrated twice to obtain the respective positions and angles. Before designing and testing the controller, the model created was tested to ensure that its response are similar to the Quad-rotor dynamics.

4.1 Control Design

The controller must ensure that the plant’s (Quad-rotor Model) output follows the reference input closely. A closed loop control structure is used in this project because it attenuated disturbances significantly and also compensate for any changes in the plant. Uneven weight distribution of Quadrotor can also be compensated by closed loop feedback.

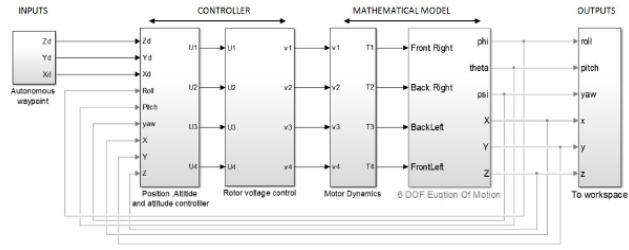


Fig. 10 Simulink Model of Quad-rotor

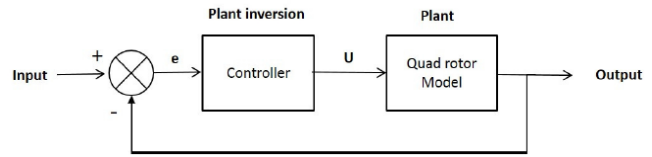


Fig. 11 Closed loop Control

The closed loop controller has to maintain output close to the input. Inherently closed loop control performs an inverse of the plant dynamics. Since the dynamics of the Quad-rotor is known, the controller gains can be tuned and an approximate plant inversion can be achieved. The resultant control signal ‘U’ is fed into the model to produce the desired output.

4.2 Controller Approach

Controller is constructed with PD loops. These PD loops inside the attitude, altitude and positional control generate the respective control signal.

The quad-rotor will use the Proportional Derivative controlsystem (PD) to determine its response and settling time. The PD controller is a closed loop feedback system which will use the output control signal and feedback it to the initial input signal. The difference of both signals will be calculated and adjustment will be made.

In this case, the actual position and orientation of the quadrotor (output signal) will be feedback and being compared to the desired position and orientation (input signal) which will allow the system to adjust the process control input accordingly.

Control error is expressed as

$$e(t) = r(t) - y(t)$$

where $e(t)$ is the error signal. $r(t)$ is the input signal and $y(t)$ is the output signal.

Proportional Control

The proportional term depends only on the control error. It can control any stable plant. Increasing the proportional gain will decrease the response time of the control system. However, if the proportional gain is too high, oscillation will occur and system will become unstable. The proportional term is given by:

$$u(t) = K_p e(t)$$

where $u(t)$ is input signal to the plant. K_p is the proportional gain and $e(t)$ is the error signal.

Derivative Control

The derivative term gives a decreasing output if the process variable is increasing. It acts on the rate of change of the error. Increasing the derivative term will cause the system to react strongly to the changes in the error and therefore increase the speed of the system response. The derivative term is given by:

$$u(t) = K_d d[e(t)]/dt$$

where K_d is the derivative gain.

PD Tuning

In order to determine value of K_p and K_d , it is required to tune the controller until it reaches the desired response. The tuning of the proportional and Derivative values is achieved using Ziegler-Nichols Method and in most cases through manual tuning and trial and error. There is also a Simulink function to automatically tune the values, but further tuning is still required to obtain satisfactory response.

4.3 Control Architecture

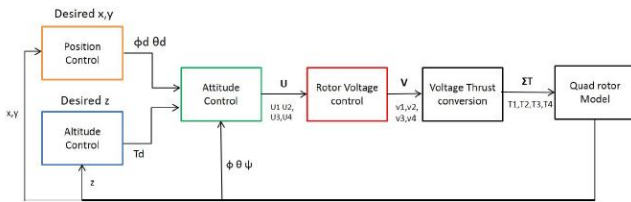


Fig. 12 Control Architecture

Roll, pitch and yaw are controlled by Inner PD loops, while the altitude and positions are controlled by the outer PD loop. The outer loop produces the desired values for the inner loop. Following section will focus into each control blocks in detail.

4.3.1 Attitude Control:

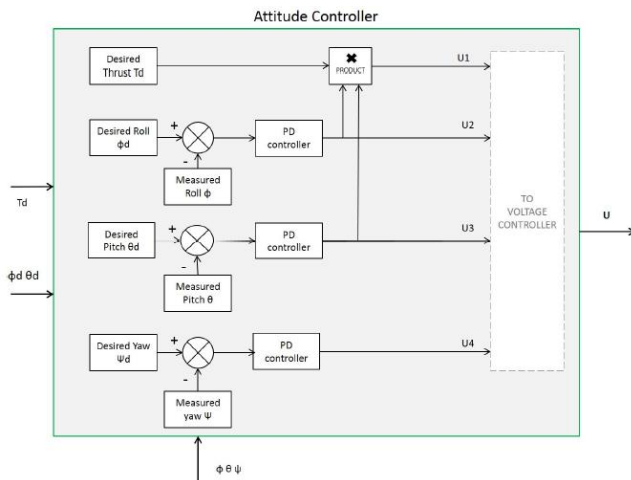


Fig. 13 Inner loop -Attitude Control

This inner loop is responsible for the control of Roll, Pitch and yaw. In this project, Quad-rotor is assumed to be symmetric about xy axes i.e. the pitch and roll controls are almost similar. Pitching down moves the Quad-rotor forward along X -axis while Rolling moves it side wards.

ROLL: The Control signal $U2$ is generated from the roll error fed through a PD control. This signal holds the roll attitude of the Quad-rotor.

PITCH: $U3$ is generated from the pitch error fed through a PD control. This signal holds the pitch attitude of the Quadrotor. As mentioned earlier the P&D values of roll and pitch are almost similar.

YAW: $U4$ is generated from the yaw error through a PD control. This signal holds the yaw attitude of the Quad-rotor. The measured ϕ, θ, ψ are the actual feedback values from the output of the model.

4.3.2 Autopilot:

Altitude Control

This outer loop control generates the desired thrust T_d required to lift the Quad-rotor to the desired altitude. It is manipulated from the altitude error fed through a PD controller. T_d is then passed to the attitude controller for the lift vector compensation due to roll and pitch. Hence the control signal $U1$ will hold the desired altitude of the Quad-rotor even during roll and pitch. The following block shows the control loop and the respective signals inside the altitude controller. The feedback provides the measured altitude of the Quad-rotor.

Altitude control

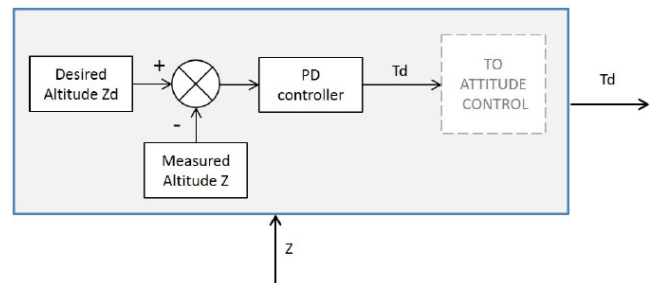


Fig. 14 Outer Loop -Altitude Control

Position control:

This outer loop generates the desired roll and pitch angle required to move the Quad-rotor to the desired X and Y positions. Feedback data from the model provides the measured X and Y . The position error signal after summing junction is fed through a PD control and it generates the desired roll and pitch angle. As mentioned earlier, its output is then fed to the attitude control to generate the control signals $U2$ and $U3$.

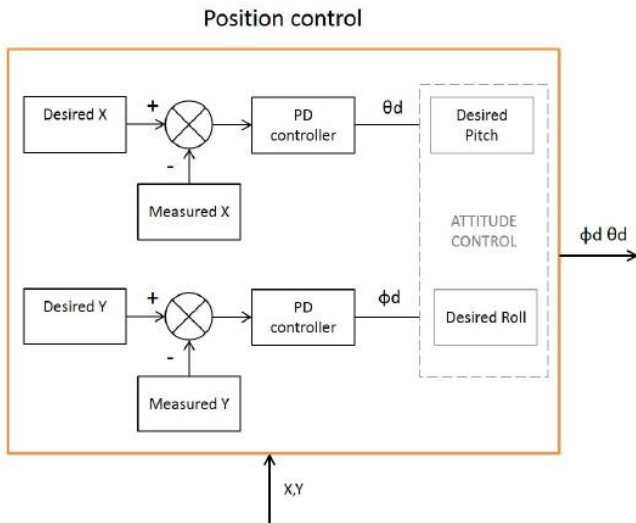


Fig. 15 Outer loop - Position control (X, Y)

simulated. The response plots clearly depict the attitude control is working as desired.

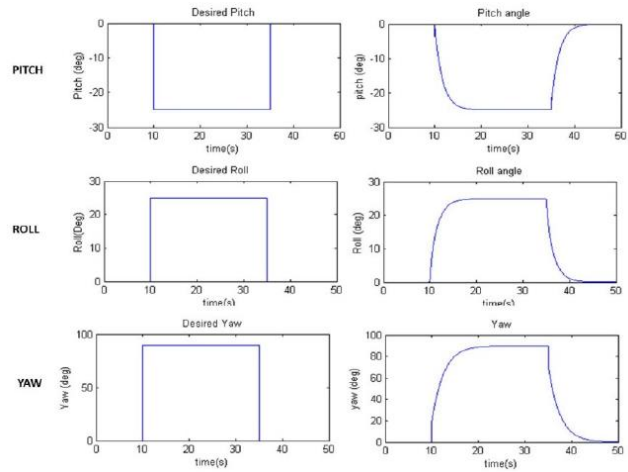


Fig. 17 Attitude control Simulation plots

4.3.3 Rotor Voltage Control:

The 4 control inputs generated by the inner and outer loops cannot be fed directly to the Quad-rotor Model because its inputs are in terms of Thrust for the 4 individual rotors. The control signals 'U' are combined to produce voltage signal for each rotor. These combinations are based on the dynamics of the Quad-rotor to exhibit the respective Flight parameter. The combinations was mentioned earlier under the Motor dynamics and also shown below in the block diagram. The output voltage 'V' is then converted to thrust by the modelled motor.

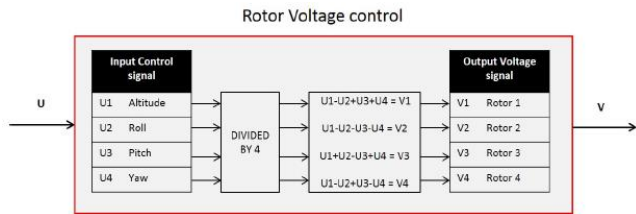


Fig. 16 Rotor voltage control

Position and Altitude Control:

A step input with a magnitude of 10 was fed to position and altitude controller. The desired 10 m input is expected to move the Quad-rotor model to 10 m position and hold. As mentioned earlier the position controller's output will command the desired roll and pitch angle to the attitude control. The right section of the plots in Fig 18 shows how the roll and pitch angles change in order to reach the desired Y and X position respectively.

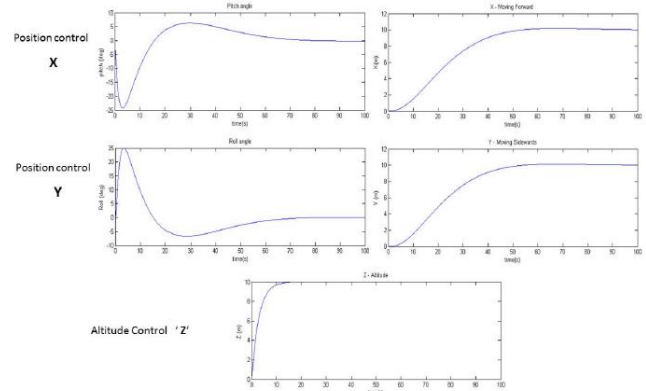


Fig. 18 Position control simulation plots

5. SIMULATIONS AND FLIGHT TEST RESULTS

The Flight test data from the Lab was captured using the Opti-track cameras and was imported into MATLAB for comparison with the simulated results. Technical difficulties and observations from comparison are also discussed.

5.1 Simulink Test Results:

Attitude control:

A pulse signal was fed as the desired Roll, pitch and yaw inputs to the designed controller for testing. The plots on the left segment in Fig 17 shows the input to the controller while the right segment shows the respective response from the model

Waypoint Navigation:

An autonomous waypoint flight was demonstrated in Simulink using the model. A set of waypoints was fed to the position controller using timer control and the respective x, y, z position data was obtained from the simulation. The waypoints and the flight path of the modelled Quad-rotor in 3D are shown below. The plots below shows that the positional controller performs as desired.

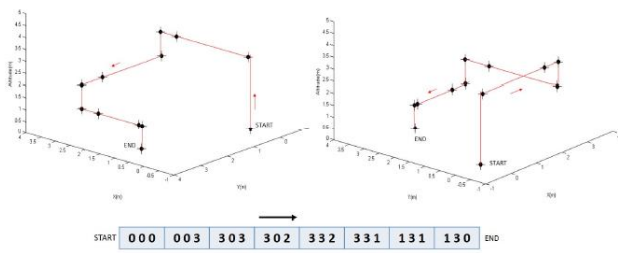


Fig. 19 3D Flight path -Waypoint Navigation using position control

5.2 Actual Flight Test

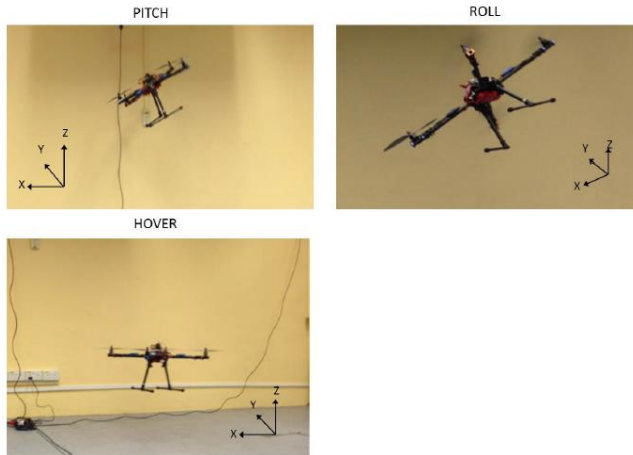


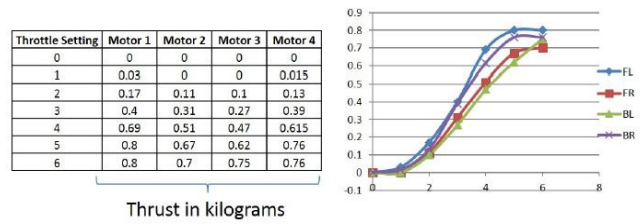
Fig. 20 Flight Test Pictures

The constructed Quad-rotor was put to flight with the Ardupilot microcontroller. The quad-rotor's movement, the positions of the quad-rotor (X, Y and Z-axis) was captured by the Opti-Track system during flight tests. The following pictures were taken during one of the actual tests. They show the pitch, roll and take off of the quad-rotor respectively during the test flight.

Technical challenges

The Quad-rotor was unstable during most of its flights. Initially the uneven weight distribution was thought to be the reason for instability. Adding counterweights, to spread the weight distribution equally, failed to solve the issue. Even trimmed flight could not completely cease the undesired yawing and rolling motion. After repeated test flights it was discovered that the motors used did not produce similar thrust though their specifications are similar.

All 4 rotors were tested using a thrust meter attached to the same ESC. The readings were taken for different throttle settings in the radio controller. The following table and the graph clearly depicts that the motors were not generating similar thrust for the same radio input. There were differences of about 100g of thrust for certain throttle settings.



Thrust in kilograms
Fig. 21 Motor Thrust Indifferences graph and Table

Simulation vs Test Flight

Besides unstable flight, certain segments of the flight test was captured well by the Opti-Track system. It was then imported into MATLAB. In Fig 22 below the plots on the right segment was captured from 3 different test flights while the plots on left segment was obtained from the Simulation performing similar outcomes of the captured data.

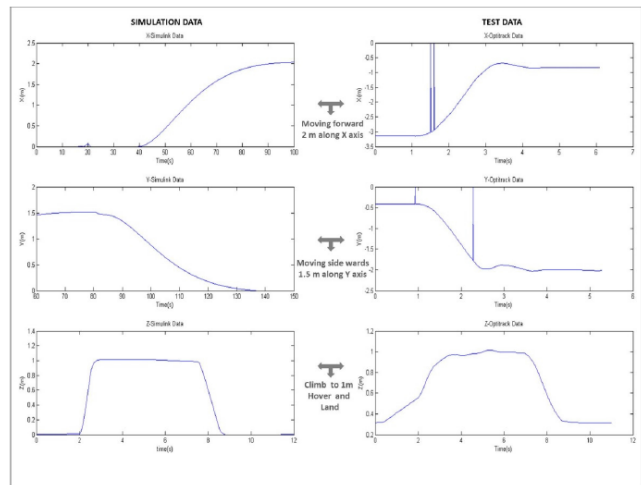


Fig. 22 Simulation v Flight Test data

From comparison the envelope of both the responses are similar with simulated response being more ideal. But the Response time of the simulation is much slower as compared to the test data. Reason being, the inputs for the actual flight test are the roll, pitch and yaw commands from the radio controller. No autopilots were used. Hence the response was fast. However, the simulation used the position controller which took longer time to compute the desired roll and pitch angles. Also the mathematical model of the system 100% similar as the actual quad-rotor and did not account for any external disturbances. These are the factors that caused the difference.

6. SWARM BEHAVIOR

Quad rotors can work in teams with the help of swarm algorithms. These algorithms are nothing but a set of rules that exhibit the three main characteristics of a swarm behaviour such as Cohesion, Separation and Alignment. The following Fig 23 provides more information about each characteristic.

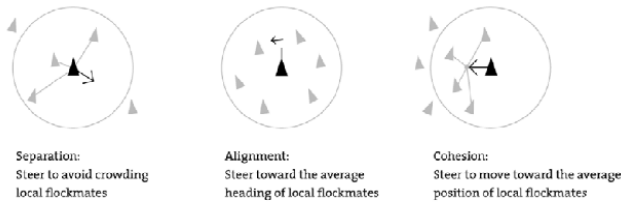


Image taken from <http://coffeepoweredmachine.com/flocking-like-its-1999/>

Fig. 23 Swarm Characteristics

6.1 Leader Follower Method

As the name describes, the leader leads a team of quadrotors. It acts as the reference point for the swarm. The actual positional information of the leader is fed into the swarm algorithm to generate the position command for the followers. The swarm algorithm makes sure that the followers are separated by a certain distance from the leader while following. The command input for each follower is computed depending on the position occupied by that follower in the formation.

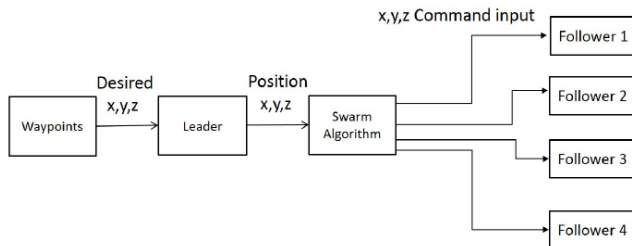


Fig. 24 Block representation of Leader Follower Method

6.2 Swarm Simulation

The position control forms the basis for swarm implementation as the output of the swarm control is in terms of positions. The capability of the position control was displayed earlier (waypoint navigation for a single quad rotor). In the following simulation, the leader is provided with the waypoints to take off and move forward. The plots in Fig 25 shows a leader and 2 followers executing the following sequence of actions.

1. Quad-rotors Take-off from their initial position.
2. The followers identify the leader and move closer to it.
3. The 2 Followers travel behind the leader as it moves forward, maintaining the safety distance predefined as separation vector in the algorithm.

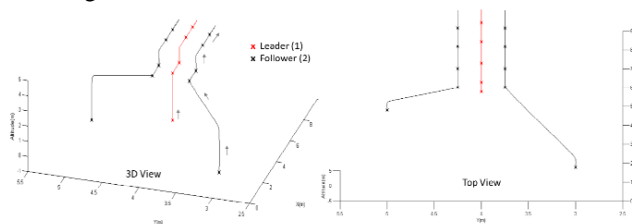


Fig. 25 Simulation Plots showing 3 Quad-rotors exhibiting swarm behaviour

The formation pattern can be changed by changing the separation vector. In the following simulation shown in fig 26, a leader and 4 Quad-rotors demonstrate different formations as they climb upwards following their leader. Leader varies his altitude only. The followers change their positions due to the varying separation vector.

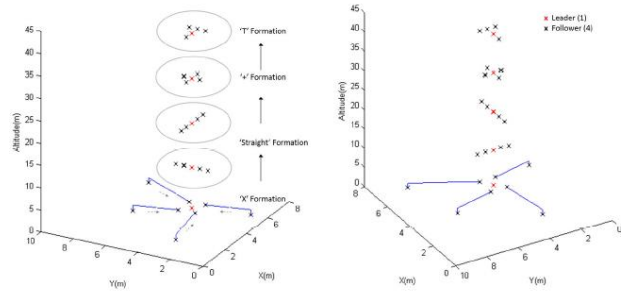


Fig. 26 Simulation plot showing a group of quad rotors changing the formation as they climb upwards.

7. CONCLUSION

This paper presented a Quad-rotor model constructed in our UGS lab and a model simulated in MATLAB. Though the simulation managed to achieve a stable and autonomous flight, the actual Quad-rotor exhibit moderate unstable controlled flight due to technical challenges mentioned earlier. Several remedial measures such as introducing the offsets to the motor to linearize the motor output failed to solve the issues.

Working with Motion capture system was completely new and knowledgeable. The ability to collect variety of flight performance data from the system without the need of additional sensors aboard the platform is greatly appreciated. From the results of both simulation and actual flight test, the students learned the limitations of simulation. This learning will improve the way we design and make our future designs more accurate and realistic.

REFERENCES

- [1] Bouabdallah, S. 2007. *Design and control of Quadrotors with Application to Autonomous Flying*. Université Aboubekr Belkaid.
- [2] Christiansen, R. S. 2004. *Design Of an Autopilot For Small Aerial Vehicles*. Brigham Young University.
- [3] M. Fadhil Abas, S. A. n.d. *Leader-Follower Formation Control of Multiple Quad-rotor Aerial Vehicles*. Chiba, Japan: Chiba University.
- [4] Soon Hooi Chiew, T. H. Go, 2012. *Swarm Coordination with Multiple Quadrotors*. Master thesis, Nanyang Technological University, Singapore.
- [5] Robert Stengel. 2012 Aircraft Flight Dynamics. [Online].
- [6] <http://www.princeton.edu/~stengel/MAE331Lecture8.pdf>
- [7] Andrew Gibiansky, "Quadcopter Dynamics, Simulation, and Control,"
- [8] Ardupilot.com. n.d. APM Open source autopilot. [online] Available at: <http://ardupilot.com/>
- [9] Copter.ardupilot.com. n.d. APM 2.5 and 2.6 Overview. [online] Available at: <http://copter.ardupilot.com/wiki/common-25-and-26-overview/>

- [10] Douglas, S. n.d. APC Propellers, props for model airplanes. [online] Available at: <http://www.apcprop.com/v/index.html>
- [11] Foxtechfpv.com. 2014. TMOTOR MT2212 KV980. [online] Available at: <http://www.foxtechfpv.com/tmotor-mt2212-kv980-p-656.html>
- [12] Hefny, M. 2012. Technical Adventures: QuadCopter Stabilization & Control System "X & Plus Configuration". [online] Available at: <http://technicaladventure.blogspot.sg/2012/09/quadcopter-stabilizationcontrol-system.html>
- [13] Icharger.co.nz. 2011. Introduction To Lipo Batteries. [online] Available at: <http://www.icharger.co.nz/articles/ArticleId/6/Introduction-To-Lipo-Batteries.aspx>
- [14] Platinum Label Lipo Docier. n.d. [e-book] Revolectrix. p. 5. http://revolectrix.com/support_docs/item_1406.pdf
- [15] Code.google.com. 2012. APM2RC - arducopter. [online] Available at: <https://code.google.com/p/arducopter/wiki/APM2RC>
- [16] Aerospace.illinois.edu. n.d. UIUC Propeller Data Site. [online] Available at: <http://aerospace.illinois.edu/m-selig/props/propDB.html>
- [17] Beikrit, S., Falaschini, C., Abdolhosseini, M. and Capotescu, F. n.d. *Qball Quadrotor Helicopter*. [report].
- [18] C.Cody, B. 2012. *Simulation and Position Control of a Quadrotor UAV*. [report].
- [19] Angeletti, G., Valente, J. R. P., Locchi, L. and Nardi, D. n.d. *Autonomous Indoor Hovering with a Quadrotor*. [report].
- [20] Cavalcante Sá, R., C. De Araújo, A. L. and T. Varela, A. 2013. *Construction and PID Control for Stability of an Unmanned Aerial Vehicle of the Type Quadrotor*. [report].
- [21] Cutler, M. J. 2010. *Design and Control of an Autonomous Variable-Pitch Quadrotor Helicopter*. [report].
- [22] Hussein, W. M., El-Khatib, M. M., Elruby, A. Y. and Haleem, H. M. n.d. *Quad Rotor Design, Simulation and Implementation*. [report].
- [23] Kim, J., Kang, M. and Park, S. 2009. *Accurate Modeling and Robust Hovering Control for a Quad-rotor VTOL Aircraft*. [report]. 43
- [24] Orsag, M. and Bogdan, S. n.d. *Influence of Forward and Descent Flight on Quadrotor Dynamics*. [report].
- [25] Palm, J., Nelson, A. and Bradford, A. 2010. *Quad-Rotor UAV project*. [report].
- [26] Raza, S. A. and Gueaieb, W. n.d. *Intelligent Flight Control of an Autonomous Quadrotor*. [report].
- [27] Roberts, J. F., Stirling, T. S., Zufferey, J. and Floreano, D. n.d. *Quadrotor Using Minimal Sensing For Autonomous Indoor Flight*. [report].
- [28] Tobias, P., Krogstad, T. R. and Gravdahl, J. T. n.d. *UAV Formation Flight using 3D Potential Field*. [report].
- [29] Elkaim, G. H. and Kelbley, R. J. n.d. *A Lightweight Formation Control Methodology for a Swarm of Non-Holonomic Vehicles*. [report].
- [30] Flyingmachinearena.org. n.d. *Flying Machine Arena*. [online] Available at: <http://flyingmachinearena.org/>
- [31] Kushleyev, A., Mellinger, D. and Kumar, V. n.d. *Towards A Swarm of Agile Micro Quadrotors*. [report].
- [32] Yasir Amir Khan Niazi. 2010. *Modeling and neural control of quadrotor helicopter*. Berlin: LAP Lambert Academic Pub.
- [33] Putro, I., 2011. *Modeling and control simulation for autonomous quadrotor*. 1st ed. Saarbrücken: LAP Lambert Academic Pub